High Internal Phase Water-in-Oil Emulsions and Related Microemulsions Studied by Small Angle Neutron Scattering. 2. The Distribution of Surfactant

Philip A. Reynolds, Elliot P. Gilbert, and John W. White*

Research School of Chemistry, The Australian National University, Canberra ACT 0200, Australia

Received: January 26, 2001; In Final Form: April 11, 2001

We have examined isotopically substituted concentrated emulsions and related microemulsions by small angle neutron scattering (SANS). The emulsions have 90% internal phase micron-scale water droplets in a continuous hexadecane microemulsion. The surfactants have polyisobutylene oligomer tails with acid−amide headgroups. Dilution experiments with surfactant concentration varying over a 75-fold range confirm that the oil phase component of the emulsion contains reverse spherical micelles. We have produced single phase samples of microemulsions designed to have the same composition and same high Q scattering as the oil phase within our emulsions. SANS data from these fit to a model with a compound micelle in which a core region of radius a little less than 15 Å is surrounded by a shell of ca. 20 Å thickness. There is no hexadecane in the core and no water in the shell. The overall volume percentages in the surfactant concentrated microemulsions of water, hexadecane, and surfactant are 6%, 31%, and 64%, while for the more dilute microemulsions we obtain 3%, 37%, and 60%. The dilution data show that the surfactant loading at the oil−water interface is almost independent of dilution, and at the highest concentrations only 5% of the surfactant is at the emulsion droplet interface, the rest being in the form of micelles. The headgroup area per molecule at the interface is 140 $Å^2$ and corresponds well with that expected for a monolayer of surfactant. The aqueous−oil interface is rough, with the water−surfactant interface smoother than the very rough surfactant−oil interface.

Introduction

Emulsions are both important and have been studied by many techniques,[1] but there has been little investigation by small angle neutron scattering (SANS) to probe structure at the nanometer scale. Water-in-fluorocarbon high internal phase emulsions have so been studied,[2,3] and there is a recent study of a dilute oil-in-water emulsion.[4] In a previous paper[5] we presented SANS results from aqueous/hydrocarbon high internal phase emulsions, a two-phase system. These were directed at the microstructure within the aqueous and/or oil regions and at the nature of the interface between them. Both the oil-rich region and the water-rich regions are of interest. The results were extensively discussed in relation to the large amount of previous work on chemically unrelated single phase microemulsions.

In our first experiments the neutron scattering contrast was varied between the constituents to selectively identify the scattering from different components of the emulsion structure. Three isotopically substituted series of concentrated emulsions were examined. These all had 90% internal phase water or salt solution droplets in continuous hexadecane. The surfactants had polyisobutylene oligomer tails with mainly acid−amide headgroups but were rather disperse in tail length and headgroup (Figure 1). The SANS results could be modeled by the sum of the scattering from an assembly of micron-scale polydisperse spherical aqueous droplets and the scattering from a continuous L_2 phase hexadecane microemulsion containing small surfactant/water reverse micellar structures. The aqueous volume fraction in the whole emulsion was about 90%, greater than the 74% close-packing limit for spheres. Even so, we saw no evidence for nonsphericality of aqueous droplets due to flattening by mutual droplet interaction. This we ascribe to significant polydispersity in the size of the aqueous droplets.

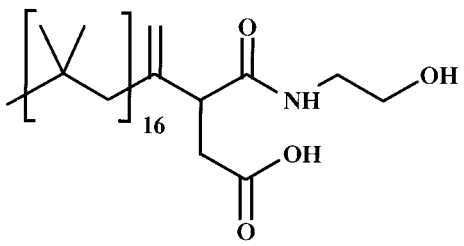

Figure 1. Typical surfactant molecule. Headgroup, exo−endo siting of carbon−carbon double bond, degree of polymerization, and isomeric nature are all variable.

The salt emulsion data fitted well to a model in which there was 12−16% of the surfactant absorbed as a monolayer at a flat [roughness of 0(3) Å] aqueous−oil interface, with the remainder as spherical 26−30 Å radius reverse micelles in the hexadecane continuous oil phase. The micelles contained 8−10% water and a large fraction of hexadecane as well as the surfactant.

The water emulsion had less surfactant absorbed at a much rougher [roughness 62(1) Å] aqueous interface and larger micelles containing more water—all reflecting less tightly held water in the aqueous as opposed to salt solution droplets.

The structure was insensitive to heating from 20 to 70 °C, but cooling to 5 °C precipitated large surfactant aggregates, giving three phases. The three possible relative specific surface areas (aqueous/aggregate, aggregate/hexadecane and aqueous/hexadecane) show increasing intrusion of the surfactant aggregate into the aqueous droplets as the aggregate increased in size.

This preliminary study was ambiguous in that although the oil phase modeling required a microemulsion structure with two

* Author to whom correspondence should be addressed. Fax: (61) 26125 4903. E-mail: jww@rsc.anu.edu.au.

10.1021/jp010349o CCC: $20.00
Published on Web 06/21/2001

length scales, three different such models could be fitted. Besides a micellar model with polydisperse spheres, a monodisperse cylindrical and a correlated lamellar model both fit equally well. This, although not often commented on, is a common result in SANS investigations.

In this paper we resolve this issue, in the classical manner, by SANS examination of a series of emulsions in which the surfactant is varied in concentration. This also allows us to measure the relative amounts of surfactant in the microemulsion and that absorbed at the oil−aqueous interface, as the concentration of surfactant changes, and to define the limits of stability of the emulsion. We now also use a newly synthesized relatively monodisperse surfactant to remove uncertainties associated with surfactant polydispersity. We shall show that spherical reverse micelles are indeed present.

We will also show that a one-phase microemulsion can be synthesized in bulk, which reproduces the oil phase in the emulsion. Further SANS studies of various such isotopically substituted microemulsions confirm the spherical micelle structure of the oil phase in the microemulsion and clarifies the micelle composition.

Last we present results showing that that these conclusions are unaffected by emulsion instability, reproducibility, and exact aqueous content and are also independent of surfactant deuteration.

Experimental Section

Surfactant. We have prepared a much more monodisperse surfactant than that used in the previous experiment. "Monodisperse" PIB or deuterated PIB were prepared by living carbocationic polymerization of isobutylene/isobutylene-d_8 and 2-chloro-2,4,4-trimethylpentane initiator in the presence of methyl chloride.[6] The protonated PIB is characterized by molecular weights (M_n) [1040 (^{1}H NMR), 930 (vapor phase osmometry), 960 (size exclusion chromatography)], polydispersity (M_w/M_n) [1.10 (mass spectrometry)], and percent exo double bond (96%). The deuterated PIB has $M_n = 1100$, $M_w/M_n = 1.11$, and exo% = 99.8%. These PIBs were used to prepare the "monodisperse" protonated and deuterated surfactants, considerably more monodisperse than our previous surfactants of dispersity 1.5−1.8. The PIB is reacted with maleic anhydride and 2-hydroxyethanolamine to give the surfactant species polyisobutylene N-(2-hydroxyethyl)succinamide (Figure 1). The final purity was checked by ^{13}C and ^{1}H NMR. The product was >95% of an equal mixture of isomers with PIB attached adjacent or one carbon removed from the carboxylic acid residue, with no detectable imide, anhydride, or hydrolysis products. The final protonated surfactant molecular volume, neutron scattering length density, and weight can be estimated as 1983 Å^3, -0.13×10^{-6} Å^{-2}, and 1113.

Preparation of Emulsions and Microemulsions. To prepare the emulsions the *n*-hexadecane (D/H mixtures) and dissolved surfactant were preheated in a water bath at ca. 80 °C and stirred as water (D/H mixtures) was added slowly over 30 s. This was followed by 5 min of rapid stirring to ensure thorough mixing.[5] This method reproducibly forms 10-g quantities of emulsion.

Dry microemulsions were prepared by dissolving surfactants into hexadecane. Wet microemulsions were formed by adding a drop of H_2O or D_2O to ca. 300 mg of dry microemulsion and leaving the preparation for several days. A clear hexadecane phase forms with a small amount of a second white, water-rich phase below. We presume the white phase is a dilute oil-in-water emulsion phase. The majority clear phase was examined by SANS. If the mixture is agitated there is a tendency toward emulsification ending in a single cloudy hexadecane phase. This process began during transport in a few samples, rendering the clear phase slightly cloudy.

SANS Experiments. SANS experiments were performed on both the LOQ instrument at the Rutherford Appleton Laboratory, United Kingdom, and the SAND instrument at the Intense Pulsed Neutron Source, Argonne National Laboratory.[49−51] For the emulsion samples the experiment and data correction and reduction were as previously described.[5] The microemulsions were run in 1 mm thick quartz cells. A total of 20 emulsion and 9 microemulsion runs will be discussed.

The emulsions were mainly contrast matched (CM), that is, the oil and aqueous phase scattering length densities are matched at high values, to contrast strongly with the low scattering length density of the surfactant. A few were contrast unmatched (UM) to highlight the aqueous droplet−oil interface. Unless otherwise specified, the emulsions had a 90−91% aqueous droplet phase content, and both emulsions and microemulsions were made up with protonated surfactant. We adopt the nomenclature H_2O, D_2O, and D/H_2O, for water, heavy water, and isotopic mixtures in the aqueous phase, and the corresponding $C_{16}H_{34}$, $C_{16}D_{34}$, and $C_{16}D/H_{34}$ for the hexadecane. The percentage figure given in the list of emulsions below is the weight percentage of surfactant in the whole emulsion or microemulsion.

The following emulsions were run: (1) $C_{16}D_{34}-D/H_2O$; CM; 4.5, 2.9, 1.8, 0.72, 0.36%; (2) $C_{16}D/H_{34}-D_2O$; CM; 0.72, 0.36, 0.20, 0.12, 0.06%; (3) $C_{16}D_{34}-H_2O$; UM; 2.9, 1.8, 0.36%; (4) $C_{16}H_{34}-H_2O$; CM; 1.6% deuterated surfactant; (5) $C_{16}D_{34}-D/H_2O$; CM; 1.45% of 95% aqueous phase; (6) $C_{16}D_{34}-H_2O$; UM; 1.45% of 95% aqueous phase.

After waiting 6 months the following emulsions were rerun without treatment: (1) $C_{16}D_{34}-D/H_2O$; CM; 2.9, 0.36%; (2) $C_{16}H_{34}-H_2O$; CM; 1.6% deuterated surfactant.

After 6 months the following emulsion had decomposed and was remixed to an apparently similar emulsion and rerun: $C_{16}D_{34}-H_2O$; UM; 1.8%. The following is the dry microemulsion: $C_{16}D_{34}$; 30, 6.5%.

The following are the wet microemulsions: (1) $C_{16}D_{34}-H_2O$; 30, 7.4%; (2) $C_{16}D_{34}-D_2O$; 30, 6.7%; (3) $C_{16}H_{34}-D_2O$; 28, 15, 7.5%.

Modeling

The scattering vector, Q, is defined as the difference between the incident and scattered neutron wavevectors. For elastic scattering, $Q = |\mathbf{Q}| = (4\pi/\lambda)\sin\theta$, where 2θ is the angle through which neutrons are scattered and λ is the neutron wavelength. All fits were performed by use of interactive IGOR[9] procedures, obtained from NIST,[10] but with some local additions. Theoretical intensities were corrected by convolution with the known resolution factors for LOQ[7] and SAND.[8] Where necessary, a refinable small flat background has been applied in the fits to account for small errors in our incoherent background correction.

We have modeled the unconvoluted total intensity as the sum of a contribution from a flat interface between the aqueous droplets and the microemulsion, a contribution from the microemulsion itself, and a flat background. Ravey et al.[11] have shown that a simple addition of intensities is appropriate, providing that the relative curvatures of the microemulsion microstructure and the interface are sufficiently different, which our previous paper established was so in this case.[5]

Uncorrelated Flat Interfaces. We can calculate the scattering from an interface consisting of an adsorbed layer of surfactant between aqueous and hexadecane phases. The formula used[5] assumes that different interfaces are mutually uncorrelated. We

have found no evidence for mutual alignment or preferred spacing of interfaces across the continuous oil-rich emulsion phase.[5] Three parameters are necessary to describe the scattering from this interface in these systems from all isotopic combinations: the specific surface of the interface (m^2/mL of emulsion), the interface roughness (Å), and the amount of surfactant absorbed at the interface (mg/m^2). For the contrast matched system on its own, only two parameters are required: roughness and the product of specific surface and the square of the surfactant amount. We note that, for large roughnesses and a small thickness of surfactant layer adsorbed, the latter is unresolvable, so we are unable to extract surfactant layer thicknesses at the aqueous interface.

Correlated Spherical Micelles. The intensity of scattering from a polydisperse uniform hard sphere fluid in the Percus−Yevick approximation with a polydispersity given by the Schultz distribution can be calculated exactly.[12] In addition to the micelle volume fraction and scattering length density difference from the continuous phase, the disposable parameters are only the micellar radius and polydispersity factor. Unlike for our previous polydisperse surfactants experiments,[5] where quite large micellar polydispersities were found, we now find with this monodisperse surfactant small polydispersities in micellar size. Thus in all cases, we have fixed the polydispersity of micelles at the reasonable and low value of 0.14—the average value obtained in several runs where this was allowed to vary.

In these experiments, unlike the previous ones,[5] we were required to model a micelle with an inner spherical core of differing scattering length density from the rest of the shell of the micelle. In particular, our microemulsion results are sensitive to the difference between the hexadecane shell and headgroup−water core of the reverse micelles. No exact solution exists for this hard sphere fluid with a complex micelle, but it may be approximated by multiplying the uniform hard sphere solution for the scattered intensity by the square of the ratio of the form factors for an isolated shell micelle and uniform sphere micelle. This requires the addition of two further parameters: core scattering length density and core radius.

By combining different isotopic substitutions with the known emulsion content and scattering length densities the water, hexadecane, and surfactant content of each of the core and shell regions within a micelle can be derived.

Results and Discussion

Emulsion Oil Phase Contains Reverse Spherical Micelles. The absolute intensity and its dependence on deuteration could be calculated for all of our previous emulsion data[5] using a model whose characteristics are (1) interfacial scattering between water droplets and the oil phase with surfactant absorbed at the interface; (2) a separation of the water−water interfaces by an oil phase averaging 1000 Å thick but very variable; (3) scattering from an assembled microstructure in the oil phase; (4) the microstructure well modeled by any of spherical inverse micelles, swollen lamellae, or rodlike micelles of finite length.

A classic way of resolving the last ambiguity is to perform a series of experiments at different surfactant concentrations. For a lamellar phase we expect the interlamellar spacing to be almost inversely linearly dependent on concentration, while the rod length in a rod phase would also be concentration dependent. However in a spherical micellar phase we expect the distance parameters in the structure to be almost invariant, with only the volume fraction of micelles varying strongly. The best emulsions to test this on are contrast-matched ones in which the aqueous−oil interface scattering is minimized by matching the aqueous phase scattering length density to the mean oil phase scattering length density. In that case we observe scattering from the reverse micelles together with that from surfactant adsorbed at the oil−aqueous interface.

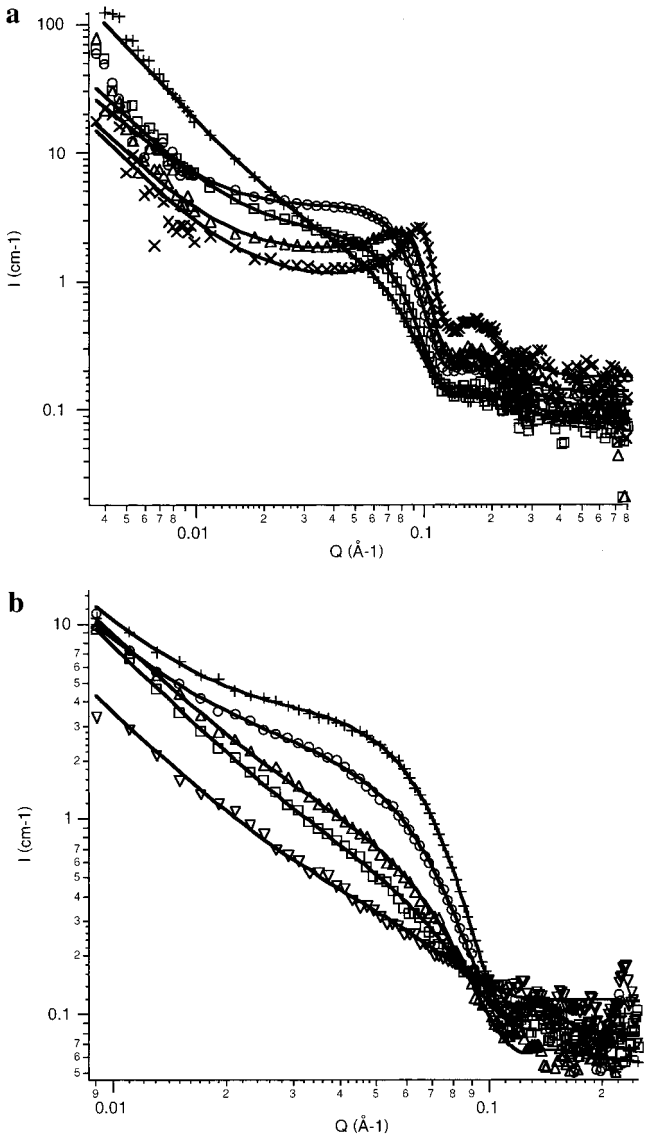

Figure 2. (a) Small angle neutron scattering for five emulsions at 20 °C illustrating the change with surfactant dilution at higher surfactant concentrations. The highest surfactant concentration is × (4.5 wt % surfactant), then triangles (2.9%), circles (1.8%), squares (0.72%), and + (0.36%). Figure 2b SANS for five emulsions at 20 °C illustrating change with surfactant dilution at lower surfactant concentrations. The highest surfactant concentration is + (0.72%), circles (0.36%), upright triangle (0.20%), square (0.12%), and inverted triangle (0.06%).

Figure 2a shows five such contrast-matched scattering curves for emulsions obtained with SAND, with surfactant concentration varying from 4.5% (the highest we have been able to produce in a 90% aqueous emulsion) to 0.36%. They are fitted with the same model, whose parameters—transformed to physically meaningful parameters—are shown in Table 1. For the concentrated surfactant samples, the interfacial roughness when refined had large errors, since the micellar scattering dominates. Thus, we fixed the interfacial roughness at 25 Å, the mean value. Figure 2b shows a more dilute series varying from 0.72 to 0.06% obtained with LOQ. The fitted results are shown in Table 2. As opposed to the concentrated surfactant emulsions, here the interfacial scattering dominates. Accordingly, we have fixed the

TABLE 1: Structural Parameters Derived from Fitting the Surfactant Concentrated Emulsion Data

surfactant concentration (%)	4.5	2.9	1.8	0.72	0.36
microemulsion, micelle radius (Å)	31.6(1)	31.9(1)	32.4(2)	31.9(3)	32.3(8)
surfactant volume fraction in micelle	0.83(1)	0.74(1)	0.79(3)	0.83(9)	0.80
water volume fraction in micelle	0.056(4)	0.032(4)	0.02(1)	0.01(1)	−
volume fraction of micelles in oil phase	0.463(2)	0.314(3)	0.140(6)	0.077(1)	0.034(5)
surfactant absorbed at interface (mg/mL)	2.6(1)	1.17(7)	0.95(5)	0.97(4)	−
fraction of total surfactant absorbed at interface	0.06	0.04	0.05	0.13	−

TABLE 2: Structural Parameters Derived from Fitting the Surfactant Dilute Emulsion Data

surfactant concentration (%)	0.72	0.36	0.20	0.12	0.06
microemulsion, micelle radius (Å)	37.9(1)	37.1(3)	33.6(8)	31.9(11)	29.7(35)
volume fraction of micelles in oil phase	0.068(1)	0.035(1)	0.018(4)	0.013(5)	0.007(7)
interface roughness (Å)	63(5)	36(5)	32(10)	32(16)	28(35)
surfactant absorbed at interface (mg/mL)	1.5(1)	1.20(6)	1.56(5)	1.41(5)	0.62(6)
fraction of total surfactant absorbed at interface	0.21	0.33	0.78	1.17	1.03

volume fraction of surfactant in each micelle at 89% of the micelle volume, the mean of the values obtained on refinement for all five samples. Both sets of fits are good.

There is some overlap of the two data series, and the relatively good agreement of the curves and derived parameters for 0.72% and 0.36% is encouraging, given that the two series of emulsions were produced in two separate batches, with surfactant from two different preparations, measured on different instruments with differing resolutions, with differing time lags after preparation.

As discussed below there is some evidence that the hexadecane, or an impurity within it, promotes emulsion formation. The protonated hexadecane used was 99+% pure and the deuterated 98% pure, so any surfactant within the hexadecane is much less than 2% (corresponding to much less 0.2% in the emulsion mix, given the 90% aqueous fraction). We assume most impurities are neighboring alkanes. Nevertheless, we confirmed by experiment that neither protonated nor deuterated hexadecane with no added surfactant formed an emulsion with water.

Tables 1 and 2 show that the micellar radius is unchanged at 30−37 Å over the entire range of concentrations used, corresponding to micellar volume fractions in the oil phase of 0.46 down to 0.007, almost 2 orders of magnitude. This confirms that the reverse microemulsion mainly contains spherical micelles. Figure 3 shows the relation between the total amounts of surfactant detected in the scattering experiment and the total actually added in the emulsion mix. We will further discuss the oil-phase constitution when we present the microemulsion results below.

Surfactant at the Aqueous-Oil Interface. The three contrast-unmatched emulsions were fitted to our standard model to extract the surface area of the oil−aqueous interface. The 2.9% sample gave 0.66(1) m^2 mL^{-1}; the 1.8%, 1.08(1) m^2 mL^{-1}; and the 0.36%, 1.03(1) m^2 mL^{-1}. These values are slightly larger than those observed previously with impure surfactant (0.58−0.71). The roughness values observed, 72, 116 and 133 Å, are also larger. There appears to be a correlation; the larger the surface area produced in our standard mechanical preparation, the larger is the roughness.

We can use these results to obtain a measure of the surfactant adsorbed at the aqueous−oil interface. This is listed in Tables 1 and 2. Although there is a suggestion that at the very highest concentration this value is larger, and at the smallest, smaller, the major feature of these results is the constant value of the adsorbed amount, which remains the same over almost a 100-fold dilution. The mean amount adsorbed corresponds to 140 $Å^2$ per molecule at the aqueous−oil interface. This corresponds well with the 90−120 $Å^2$ found by isotherm and reflectometry

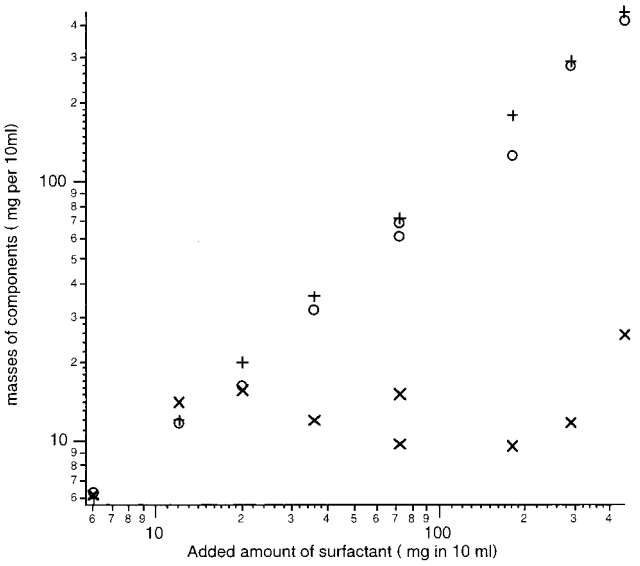

Figure 3. Surfactant distribution: total added (+); SANS measurement of microemulsion content (O); SANS measurement of surfactant adsorbed at the aqueous/oil interface (×).

measurements at the air−water interface.[13] We can conclude that, as expected, the aqueous−oil interface is stabilized by a monolayer of surfactant and that this surfactant is tightly bound compared to that in the micelles. We also notice that only at the very highest dilution is more than a small fraction of the surfactant adsorbed at the aqueous−oil interface. Thus multilayer formation is not thermodynamically favored. This might be expected if the major stabilization of the surfactant at the interface is by hydration of the headgroup.

The roughness observed in the contrast unmatched data corresponds to the roughness at the interface of oil with the remainder, i.e., surfactant plus aqueous phase. For the contrast matched data the roughness reflects the interface between surfactant and either oil or water. Thus, these two roughnesses are not necessarily the same. Indeed, we observe about 30 Å for the latter, substantially less than the ca. 100 Å for the former. We can interpret this as telling us that the water−surfactant headgroup interface is much smoother than the surfactant tail−hexadecane interface. One microscopic model for this is that a roughness on the oil side of the interface is contributed to by absorption and budding off of micelles from the interface itself. Our data are not fully fitted at the low Q range, where this effect occurs, but this does not justify a more complex model. USANS and dynamic measurements would be more informative.

The Micellar Composition and Structure from Model Microemulsions. Figure 4 shows the scattering from a contrast-

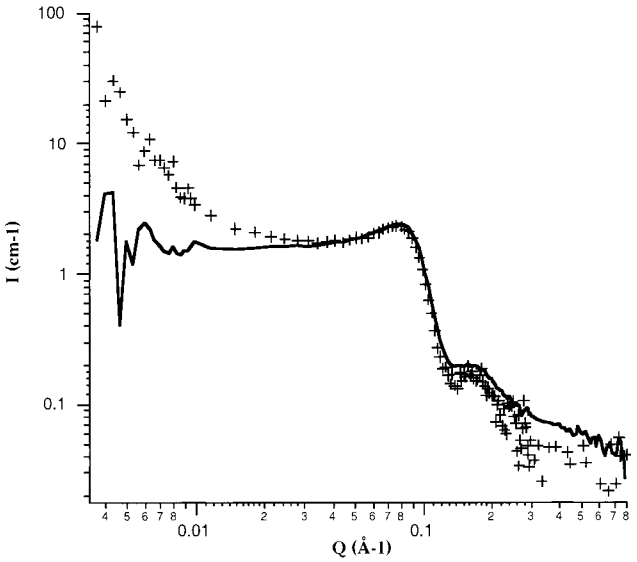

Figure 4. Comparison of scattering from emulsion (+) and a matching microemulsion (solid line).

matched emulsion in which the surfactant weight fraction is 0.029. Superimposed is the scaled scattering from a corresponding microemulsion. For an oil phase volume fraction in the emulsions of 10%, the exactly corresponding microemulsion would contain 29% surfactant and would have a scale factor of 0.1. When we use more exact numbers obtained from the known compositions and fitted contents, disussed further below, we obtain an expected scale factor of 0.13, in reasonable agreement with the observed 0.17.

We infer that the scattering at higher Q values does indeed arise from the microemulsion and that we can produce this microemulsion by the procedure outlined above. Our modeling suggests that the excess emulsion scattering at lower Q values arises from the aqueous−oil interface, which is of course absent in the microemulsion. The ability to eliminate this scattering allows us to examine the microemulsion structure in much more detail.

In Figure 5a we show four scattering patterns from differently treated microemulsions all with ca. 30% surfactant concentration. Figure 5b shows the same for ca. 7% concentration.

The crosses are surfactant−$C_{16}D_{34}$ mixtures. This will highlight surfactant micelles in a dry mixture. Triangles are surfactant−$C_{16}D_{34}$−H_2O microemulsions in which hexadecane contrasts with the rest. Circles are surfactant−$C_{16}D_{34}$−D_2O microemulsions in which surfactant contrasts with the rest. Squares are surfactant−$C_{16}H_{34}$−D_2O microemulsions in which water contrasts with the rest. Because of the absence of interface scattering, except in the case where some small emulsification occurred (see Experimental Section), the nature of the micelles and their content are much better defined than in the emulsions. In particular, we notice that the last contrast, water against the rest of the microemulsion, would in an emulsion be completely swamped by the intensity of scattering from an aqueous−oil interface of H_2O−$C_{16}D_{34}$.

The first point that we notice is that all the clear microemulsions, within the experimental errors, have intensities independent of Q at low Q. This is strong evidence for a spherical microstructure in the microemulsion, i.e., spherical reverse micelles, both in wet and dry microemulsions. We have fitted the scattering from all eight patterns (leaving out low Q regions affected by emulsification in one) to models of spherical micelles containing a spherical core of differing scattering length density.

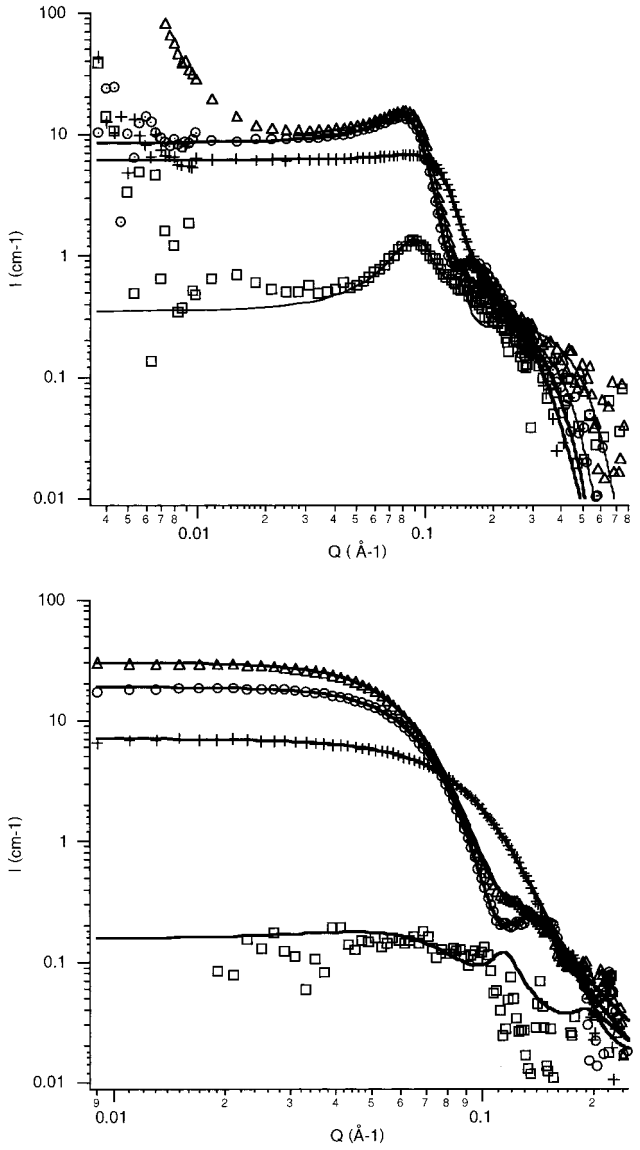

Figure 5. (a) scattering from four microemulsions with ca. 30% surfactant composition: + (dry, $C_{16}D_{34}$); square (D_2O, $C_{16}H_{34}$); circle (D_2O, $C_{16}D_{34}$); triangle (H_2O, $C_{16}D_{34}$). Fits are solid lines (triangles Q > 0.026 Å-1). (b) Scattering from four microemulsions with ca. 7% surfactant composition: + (dry, $C_{16}D_{34}$); square (D_2O, $C_{16}H_{34}$); circle (D_2O, $C_{16}D_{34}$); and triangle (H_2O, $C_{16}D_{34}$). Fits are solid lines.

The core radius consistently refined to 10−15 Å. This corresponds to such high Q values, compared to the extent of the data, that strong correlation with the core scattering length density occurs and there is a corresponding scatter in the core radius with large (1−2 Å) esds. Thus, the core data show (1) that the core radius is smaller than ca. 15 Å and (2) that the total amount of scattering in the core is well-defined. Accordingly, we fixed all core radii at 13 Å and refined only the core scattering length density. The results are listed in Tables 3 and 4 for the 30% and 7% data, respectively, and line fits to the scattering functions are shown in Figure 5.

The micelle polydispersities are small, though the dry microemulsions are slightly more polydisperse. The dry microemulsions have radii of about 22 Å but on absorption of water swell to either 31 or 38 Å. It is curious that the emulsion data of Table 1 also appear to cluster at these two values. There appears to be no obvious correlation between batch, surfactant source, or sample age. We will discuss changes in micellar radii in the next paper of this series.

TABLE 3: Structural Parameters Derived from Fitting the Concentrated Surfactant Microemulsion Data[a]

isotopic composition of oil and water	$C_{16}D_{34}$, dry	$C_{16}D_{34}-H_2O$	$C_{16}H_{34}-D_2O$	$C_{16}D_{34}-D_2O$
micelle radius (Å)	21.56(6)	30.46(4)	31	31.21(4)
micelle polydispersity	0.272(2)	0.168(2)	0.166	0.164(1)
volume fraction of micelles	0.327(3)	0.327(2)	0.33	0.332(1)
scattering length density of shell	2.30(2)	2.29(1)	0.10(1)	2.47(1)
scattering length density of core	2.58(6)	2.24(6)	4.87(6)	3.82(6)

[a] Parameters without estimated standard deviations were fixed from other sources

TABLE 4: Structural Parameters Derived from Fitting the Dilute Surfactant Microemulsion Data[a]

isotopic composition of oil and water	$C_{16}D_{34}$, dry	$C_{16}D_{34}-H_2O$	$C_{16}H_{34}-D_2O$	$C_{16}D_{34}-D_2O$
micelle radius (Å)	23.0(9)	38.4(2)	38.4	38.5(2)
micelle polydispersity	0.25(3)	0.136(5)	0.14	0.191(4)
volume fraction of micelles	0.085(15)	0.091(2)	0.0915	0.092(2)
scattering length density of shell	2.8(2)	2.94(3)	0.32(2)	2.46(4)
scattering length density of core	2.7(5)	3.0(3)	4.45(5)	3.81(6)

[a] Parameters without estimated standard deviations were fixed from other sources.

The most interesting quantity to be derived is the micellar composition, which can be obtained from the micellar scattering length densities and those for the pure components.[5]

The dry micelles contain 36(1)% by volume of hexadecane for the "30%" microemulsions and 43(3)% for the "7%" one. The slight increase in hexadecane content on micellar dilution is expected on general thermodynamic grounds. The slight excess in scattering length density of the core over the shell may reflect two factors. First, the scattering length density of the headgroup can be estimated at 2.1×10^{-6} Å^2, substantially more than the -0.35 of the PIB tail due to the presence of oxygen and nitrogen nuclei and the relative lack of hydrogens. Second, hexadecane could be predicted to be excluded from the core, due to the core's polarity. The observed core SLDs are consistent with both of these factors being operative. The aggregation number for the surfactant in these micelles is only 13.5 for the "30%" microemulsion and 14.6 for the "7%" one.

The $C_{16}H_{34}-D_2O$ wet microemulsion data reveal that the water is almost exclusively in the core region, giving a high core SLD and a shell SLD characteristic of protonated hydrocarbon. Both the $C_{16}D_{34}$ microemulsions have similar and intermediate shell scattering length densities, indicating again no water content in the shell and substantial hexadecane content. The core SLD of the $C_{16}D_{34}-D_2O$ data is greater than for the $C_{16}D_{34}-H_2O$ data, indicating water content in the core, and the intermediate value reflects the factors noted for the dry emulsion cores. There are six fitted SLDs for each system and only four independent volume fractions, water and hexadecane in shell and core. These are reasonably self-consistent and can be interpreted for the "30%" data as 6% of water in a small core by volume in the micelles, 31% hexadecane, and 64% surfactant in a surrounding shell. The "7%" data gives 3%, 37%, and 60%. There is no significant volume fraction of water in the PIB/hexadecane shell region and, conversely, little hexadecane in the core surfactant headgroup region.

We can transform these numbers to give 2.0 and 2.5 hexadecane molecules per surfactant molecule and 7.1 and 3.6 water molecules per surfactant molecule. There are 40 and 72 molecules of surfactant per micelle. The statistical errors in all these numbers are 1−2%, but we should recognize that systematic errors are more significant.

We can compare the 64% surfactant content found in the concentrated microemulsion with the 74% found in the emulsion fitting—the agreement is satisfactory but gives a better idea of the true errors. The emulsion data also indicate, but with poor accuracy, that the micelles do contain water, with relatively more water in the more surfactant concentrated systems. In the previous paper,[5] fitting to a water−hexadecane emulsion stabilized by a very polydisperse surfactant gave a surfactant content of only 33%, with hexadecane 43% and water 24%. The micelles were of similar size to these but much more polydisperse. We might expect both the water and particularly hexadecane content to be larger in micelles in which the polydispersity of the surfactant causes much more inefficient packing.

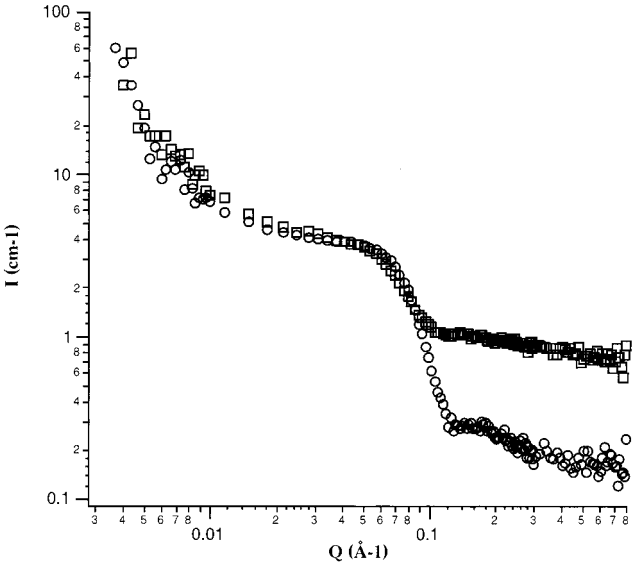

Figure 6. The scattering from an emulsion consisting of $C_{16}H_{34}$, deuterated surfactant, and a mainly H_2O contrast-matched water phase (squares) with that from of $C_{16}D_{34}$, protonated surfactant, and a mainly D_2O contrast-matched water phase (circles).

Range of Validity of These Conclusions. *(A) Deuteration.* We have implicitly assumed that all available information from isotopic substitution can be obtained solely by use of protonated surfactant and that complete inversion of the D/H substitution does not affect the coherent part of the small angle scattering. We have tested this by comparing the scattering from an emulsion consisting of $C_{16}H_{34}$, deuterated surfactant, and a mainly H_2O contrast-matched water phase with that from of $C_{16}D_{34}$, protonated surfactant, and a mainly D_2O contrast-matched water phase with the same surfactant content. As shown in Figure 6, these are very similar, apart from a higher incoherent background in the former, expected because of its higher overall proton content. We can conclude that, for these *single* surfactant emulsions, the use of necessarily large quantities of deuterated surfactant is unnecessary—all useful information can be extracted using protonated surfactants alone.

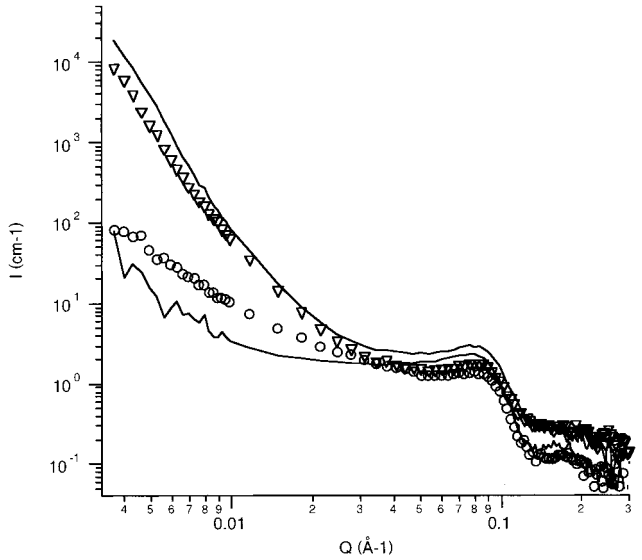

Figure 7. Scattering from 95% aqueous phase emulsions: circle, contrast-matched; triangle, contrast-unmatched. Solid lines are the corresponding 90% aqueous scattering results for the same surfactant−oil ratio.

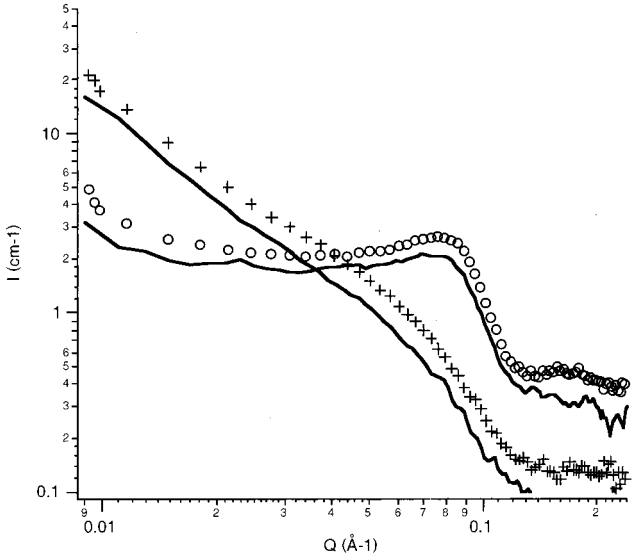

Figure 8. Scattering from typical emulsions 2 weeks after preparation (circles and crosses) and 6 months after preparation (solid lines)

(B) Aqueous Phase Content. Figure 7 illustrates the contrast-matched and -unmatched runs for emulsions with 90% and 95% aqueous content and the same surfactant-to-hexadecane ratios. It can be seen that the changes are not large. If we fit all four datasets with the model, we conclude that there are no large changes in the microemulsion structure: the micellar radius is 29.8(1)−32.2(1), the micellar volume fraction 0.26−0.32, and the SLD difference from the $C_{16}D_{34}$ similar in each of the pairs of comparable 90/95% runs.

There are some slight differences in the aqueous−oil interfaces, though. For the 90% data, we obtain a specific surface area of 0.66 m^2 mL^{-1} and a surfactant surface loading of 1.2 mg mL^{-1}.

For the 95% data we obtain figures of 0.22 and 2.9. A given mechanical treatment produces a smaller surface area, but a larger amount of surfactant is absorbed at the interface. It would appear the emulsification process is less well advanced in the 95% data, analogous to our previous results for calcium nitrate based emulsions, where we showed that the more effective the mechanical treatment, the larger the surface area.

(C) Aging Effects. We have examined again four emulsions after they have aged for 6 months. While to the naked eye they had not changed, the SANS before and after showed that both the micellar content and the interface surface loading decreased by 16−40%. Figure 8 illustrates this for a pair of emulsions.

We notice that the incoherent background is also decreasing. A simple explanation for this is that surfactant—the major protonated component—is slowly removed from the emulsion by slow chemical reaction, so the surfactant content in the emulsion is decreasing. A simple destruction of surfactancy in the molecule by slow reaction is not sufficient. A combination of this surfactant removal and a decrease of aqueous−oil interfacial area by Ostwald ripening—noting the constant per square meter coating of this interface by surfactant—would account for both interfacial and micellar surfactant contents decreasing.

We were surprised that Ostwald ripening did not proceed much more rapidly, leading to emulsion decomposition in all cases, although this did sometimes occur. We took one such completely separated emulsion and remixed it in the standard way. An emulsion of normal appearance reformed. The SANS showed the original aqueous−oil surface area was recovered; i.e., the droplet size was recovered. However there was a 40% loss in micelle volume fraction in the oil phase, corresponding to the slow surfactant loss noted above.

Conclusion

All these emulsions of changing surfactant, water content, and age possess the same generic structure, with only minor changes in the continuous oil microemulsion phase and at the interface of this with the micron-sized aqueous droplets.

The two series of dilution experiments, in which surfactant concentration in the emulsions has been varied over a 75-fold range, fit a model in which the microemulsion contains reverse spherical micelles. The insensitivity of the micellar radius and content to dilution is a classic indicator that the structure is indeed spherical rather than lamellar or rodlike. It is remarkable that only 0.06 wt % of surfactant enables production of an emulsion stable over weeks if not months.

We have produced single-phase samples of a microemulsion designed to have the same composition as the oil phase within an emulsion. The scattering at higher Q, in the range where microemulsion scattering dominates the total emulsion scattering in our model, is almost identical for both emulsion and microemulsion, indicating that both have very similar structure in the length scales sampled by SANS.

The SANS from microemulsions of two surfactant concentrations each of four different isotopic composition has been examined. They clearly show the constant intensity at low Q expected from a spherical micellar system and the data fit to a model with a compound micelle in which a core region of radius a little less than 15 Å is surrounded by a shell of ca. 20 Å thickness. We can determine the hexadecane, surfactant, and water composition in the core and shell regions. There is no hexadecane in the core and no water in the shell. The overall volume percentages in the surfactant concentrated microemulsions of water, hexadecane, and surfactant are 6%, 31%, and 64%; while for the more dilute we obtain 3%, 37%, and 60%. These surfactant contents are much higher and the polydispersity in micelle size much smaller than our previous work with much more polydisperse surfactant.

The dilution data also reveal that the surfactant loading at the oil−water interface is almost independent of dilution, and

at the highest concentrations only 5% of the surfactant is at the interface; the rest is in the form of micelles. The headgroup area per molecule at the interface is 140 Å^2, corresponding well with that found at the air−water interface (90−120 Å^2) and to a monolayer of surfactant. The aqueous−oil interface is very rough, and we can interpret the roughnesses that we observe as showing that the water−surfactant interface is much smoother than a very rough oil−surfactant interface.

Acknowledgment. We would like to thank Dr. P. Thiyagarajan and Mr. D. Wozniak at Argonne National Laboratory and Drs. R. Heenan and S. King at the Rutherford-Appleton Laboratory for experimental assistance and advice on modeling. We would also like to thank Prof. R. Faust, Harvard University, and Dr. George Adamson, ANU, for their parts in the surfactant synthesis. This work has benefited from the use of the Intense Pulsed Neutron Source at Argonne National Laboratory, which is funded by the U.S. Department of Energy, BES-Materials Science, under Contract W-31-109-ENG-38. Travel grants through the Australian Government ISTAC/ANSTO Access to Major Facilities Program are gratefully acknowledged. This work was financed by the Australian Research Council under SPIRT and SRF awards joint with ORICA and ICI UK Ltd. We would also like to thank Dr. Deane Tunaley, Dr. Richard Goodridge, and Dr. D. E. Yates of ORICA for useful discussions.

References and Notes

(1) Cameron, N. R.; Sherrington, D. C. *Adv. Polym. Sci.* **1996**, *126*, 163.

(2) Ravey, J. C.; Stebe, M. J.; Sauvage, S. *Colloids Surf. A* **1994**, *91*, 237.

(3) Langenfeld, A.; Lequeux, F.; Stebe, M. J.; Schmitt, V. *Langmuir* **1998**, *14*, 6030.

(4) Staples, E.; Penfold, J.; Tucker, I. *J. Phys. Chem. B.* (Web publication) **2000**, *104*, 606.

(5) Reynolds, P. A.; Gilbert, E. P.; White, J. W. *J. Phys. Chem. B* **2000**, *104*, 7012.

(6) Balogh, L.; Faust, R. *Polym. Bull.* **1992**, *28*, 367.

(7) Heenan, R.; King, S. In *ISIS User Guide*; Boland, B., Whapham, S., Eds.; ISIS, Rutherford Appleton Laboratory: Didcot, 1992.

(8) Thiyagarajan, P.; Urban, V.; Littrell, K.; Ku, C.; Wozniak, D. G.; Belch, H.; Vitt, R.; Toeller, J.; Leach, D.; Haumann, J. R.; Ostrowski, G. E.; Donley, L. I.; Hammonds, J.; Carpenter, J. M.; Crawford, R. K.: ICANS XIV−The Fourteenth Meeting of the International Collaboration on Advanced Neutron Sources, June 14−19, 1998, Starved Rock Lodge, Utica, Illinois, Volume 2, 864−878.

(9) IGOR Pro, Wavemetrics Inc., P.O. Box 2088, Lake Oswego, OR97035, U.S.A.

(10) Kline, S. R. Private communication.

(11) Ravey, J. C.; Sauvage, S.; Stebe, M. J. *J. Phys. IV C8* **1993**, *3*, 141.

(12) Griffith, W. L. *Phys. Rev. A* **1987**, *35*, 2200.

(13) Reynolds, P. A.; Gilbert, E. P.; White, J. W. To be published.